



**HAL**  
open science

**Ultra-high performance supercritical fluid  
chromatography hyphenated to atmospheric pressure  
chemical ionization high resolution mass spectrometry  
for the characterization of fast pyrolysis bio-oils**

Julien Crepier, Agnès Le Masle, Nadège Charon, Florian Albrieux, Pascal  
Duchêne, Sabine Heinisch

► **To cite this version:**

Julien Crepier, Agnès Le Masle, Nadège Charon, Florian Albrieux, Pascal Duchêne, et al.. Ultra-high performance supercritical fluid chromatography hyphenated to atmospheric pressure chemical ionization high resolution mass spectrometry for the characterization of fast pyrolysis bio-oils. *Journal of Chromatography B - Analytical Technologies in the Biomedical and Life Sciences*, 2018, 1086, pp.38-46. 10.1016/j.jchromb.2018.04.005 . hal-01803300

**HAL Id: hal-01803300**

**<https://hal.science/hal-01803300>**

Submitted on 25 Jul 2018

**HAL** is a multi-disciplinary open access archive for the deposit and dissemination of scientific research documents, whether they are published or not. The documents may come from teaching and research institutions in France or abroad, or from public or private research centers.

L'archive ouverte pluridisciplinaire **HAL**, est destinée au dépôt et à la diffusion de documents scientifiques de niveau recherche, publiés ou non, émanant des établissements d'enseignement et de recherche français ou étrangers, des laboratoires publics ou privés.

1     **Ultra-high performance supercritical fluid chromatography hyphenated to atmospheric**  
2     **pressure chemical ionization high resolution mass spectrometry for the characterization of**  
3                     **fast pyrolysis bio-oils.**

4  
5     **AUTHORS :** Julien CREPIER<sup>(a)</sup>, Agnès LE MASLE<sup>(a)</sup>, Nadège CHARON<sup>(a)</sup>, Florian ALBRIEUX<sup>(a)</sup>,  
6                     Pascal DUCHENE<sup>(a)</sup>, Sabine HEINISCH<sup>\*(b)</sup>

7     <sup>a</sup>*IFP Energies nouvelles, Rond-point de l'échangeur de Solaize, BP 3, 69360 Solaize, France*

8     <sup>b</sup> *Université de Lyon, Institut des Sciences Analytiques, UMR 5280, CNRS, ENS Lyon, 5 rue de*  
9     *la Doua, 69100 Villeurbanne, France*

10  
11     **CORRESPONDENCE :**

12  
13     Sabine HEINISCH  
14     E-mail : [sabine.heinisch@univ-lyon1.fr](mailto:sabine.heinisch@univ-lyon1.fr)  
15     Phone.: +33 4 37 42 35 51

16  
17     Agnès LE MASLE  
18     E-mail : [agnes.le-masle@ifpen.fr](mailto:agnes.le-masle@ifpen.fr)  
19     Phone.: +33 4 37 70 23 91

20  
21  
22  
23     **ABSTRACT**

24     Extensive characterization of complex mixtures requires the combination of powerful  
25     analytical techniques. A Supercritical Fluid Chromatography (SFC) method was previously  
26     developed, for the specific case of fast pyrolysis bio oils, as an alternative to gas  
27     chromatography (GC and GCXGC) or liquid chromatography (LC and LCxLC), both separation  
28     methods being generally used prior to mass spectrometry (MS) for the characterization of  
29     such complex matrices. In this study we investigated the potential of SFC hyphenated to high  
30     resolution mass spectrometry (SFC-HRMS) for this characterization using Negative ion  
31     Atmospheric Pressure Chemical ionization ((-)APCI) for the ionization source. The interface  
32     between SFC and (-)APCI/HRMS was optimized from a mix of model compounds with the  
33     objective of maximizing the signal to noise ratio. The main studied parameters included both  
34     make-up flow-rate and make-up composition. A methodology for the treatment of

35 APCI/HRMS data is proposed. This latter allowed for the identification of molecular formulae.  
36 Both SFC-APCI/HRMS method and data processing method were applied to a mixture of 36  
37 model compounds, first analyzed alone and then spiked in a bio-oil. In both cases, 19  
38 compounds could be detected. Among them 9 could be detected in a fast pyrolysis bio-oil by  
39 targeted analysis. The whole procedure was applied to the characterization of a bio-oil using  
40 helpful representations such as mass-plots, van Krevelen diagrams and heteroatom class  
41 distributions. Finally the results were compared with those obtained with a Fourier Transform  
42 ion-cyclotron resonance mass spectrometer (FT-ICR/MS).

43

#### 44 **KEY WORDS**

45 Ultra-High Performance Supercritical Fluid Chromatography; High Resolution Mass  
46 Spectrometry; APCI source; Biomass fast pyrolysis; Bio-oil ; Complex samples

47

#### 48 **1. Introduction**

49 Because of the necessity to develop new sources of energy for the future, the production of  
50 second generation biofuels from lignocellulosic biomass seems to be a promising option,  
51 implying different ways of conversion [1]. One of them (fast pyrolysis) consists in liquefying  
52 biomass by thermochemical process operating in the range of 400 to 450°C. This process  
53 results in bio-oils, very rich in oxygen compounds, corrosive and thermally unstable. For  
54 further uses as biofuels or bio-based products, upgrading is necessary which can be only  
55 achieved if a detailed characterization is available. Recent publications present a  
56 comprehensive overview of current analytical techniques used to characterize pyrolysis bio-  
57 oils [2-4]. It is pointed out in both papers that high resolution mass spectrometry (HRMS) has  
58 become the primary method for the analytical characterization of bio-oils, considering its  
59 potential to determine both the molecular weights and the elemental compositions of  
60 thousands of bio-oil compounds [3]. Electrospray ionization (ESI) and Atmospheric Chemical  
61 Ionization (APCI) are commonly applied ionization techniques, mostly operated in negative  
62 ionization mode. According to Stas et al. [3], a distinct advantage of negative-ion APCI is that  
63 it can detect some more unsaturated, less polar bio-oil compounds with higher carbon  
64 numbers and m/z range not detectable by negative-ion ESI. In spite of its impressive analytical  
65 power, two key issues arise from the use of HRMS as single analytical technique. Those include  
66 (i) the risk of matrix effects reducing the ionization yield and (ii) the impossibility of

67 differentiating the very large number of positional and structural isomers present in bio-oils.  
68 However both issues may be theoretically overcome if an appropriate separation technique is  
69 hyphenated to HRMS.

70 Compound identification by gas chromatography hyphenated with mass spectrometry (GC-  
71 MS) and quantification using gas chromatography and flame ionization detection (GC-FID) are  
72 commonly carried out [5]. Thanks to its high resolution power, GC and overall GCxGC make a  
73 valuable contribution to the detailed characterization of complex matrices such as bio-oils.  
74 Nearly 300 compounds could be identified by GC-MS or GCxGC-MS in fast pyrolysis bio-oils,  
75 providing a wide range of chemical families including aldehydes, ketones, aromatic esters,  
76 carboxylic acids, alcohols, carbohydrates, furans, pyrans, phenols, benzenediols,  
77 methoxyphenols, dimethoxyphenols [6]. However, without prior derivatization step, some  
78 problems may occur with molecular structures higher than around 200 g/mol including (i) low  
79 separation power with the presence of numerous coelutions even in GCxGC [4], (ii) very high  
80 retention for heavy compounds and (iii) thermal instability (e.g. for carbohydrates) leading to  
81 compound degradation in the injection unit. In addition, there may be some identification  
82 issues from usual data bases, in particular with polyfunctional and oxygenated compounds  
83 having a high number of carbon atoms. As a result, in spite of the high potential of GCxGC,  
84 alternative separation techniques are strongly required in order to provide a more  
85 comprehensive view on bio-oil composition.

86 Two-dimensional reversed phase liquid chromatography (RPLC) techniques were applied to  
87 the analysis of the aqueous fraction of a bio-oil. It was found that RPLC x RPLC had the  
88 potential of resolving up to 2000 peaks [7], highlighting the potential of this technique for the  
89 comprehensive analysis of the aqueous phase of the bio-oil. Both photo diode array (PDA)  
90 and MS detection were latter coupled to RPLC x RPLC and a more detailed analysis could be  
91 obtained [8]. Finally, an orthogonal separation system was also recently proposed involving  
92 both RPLC and, for the first time, SFC (RPLC x SFC) [9]. However in spite of promising results  
93 on the aqueous fraction, neither LC, nor SFC techniques were ever been applied to the  
94 characterization of the whole bio-oil sample.

95 In this context we guessed that SFC hyphenated to HRMS could be a more versatile analytical  
96 technique, able to provide more comprehensive information on bio-oil composition. In a  
97 previous work [10], a SFC-UV method was developed with a view to later analyzing the whole  
98 sample by SFC-HRMS. The optimization of the separation parameters was directly performed

99 on bio-oil sample in order to take into account the complexity of such a sample at the earliest  
100 stage of method development [10]. Because of CO<sub>2</sub> decompression at the outlet of SFC device,  
101 only atmospheric ionization sources such as ESI or APCI can be hyphenated to SFC. The use of  
102 SFC-ESI/MS was often reported in different application fields with simple quad or high  
103 resolution mass spectrometers [11–13]. The APCI source has been rarely used in SFC/MS but  
104 recently proposed for the analysis of natural non-polar compounds [14].

105 Our choice for the APCI source was directed by the presence of components with a very large  
106 variety of chemical and physical properties (polarity, molecular weight, chemical functionality,  
107 m/z range etc...). The selection of suitable interface parameters was based on an optimization  
108 procedure, presented in this study for the specific case of bio-oils. The large amount of data  
109 generated in SFC-HRMS for complex sample analysis makes the use of specific software  
110 necessary, especially for non-targeted analysis as for bio-oils. We therefore developed a  
111 home-made software for data processing. Its key features are presented here. The relevance  
112 of the whole approach is highlighted with a mixture of model compounds, analyzed alone and  
113 spiked in complex bio-oil matrix. The obtained results regarding bio-oil composition are  
114 discussed with the support of usual representations including mass-maps, van Krevelen  
115 diagrams and heteroatom class distribution. Finally, these results are compared to those  
116 obtained with a Fourier Transform ion-cyclotron resonance mass spectrometer (FT-ICR/MS)  
117 which is known to be the most powerful in terms of mass resolving power.

118

## 119 **2. Materials and methods**

120

### 121 *2.1. Chemicals and sample preparation*

122 Solvents (acetonitrile, methanol, water) were MS grade from Sigma Aldrich (Steinheim,  
123 Germany). Carbon dioxide SFC grade (99.97%) was purchased from Air Liquide (B50 bottle  
124 under pressure). Tetrahydrofuran (THF) was purchased from VWR (Fontenay sous bois,  
125 France).

126 36 model compounds were purchased from Sigma Aldrich (Steinheim, Germany). Their names  
127 and structures are listed in Table S1 of the supplementary information. The model mix was  
128 obtained by dissolving each compound in THF (200 mg/kg). The fast pyrolysis bio-oil was  
129 obtained from conifer sawdust, provided by IFP Energies nouvelles. It was diluted in THF (1/5  
130 w/w) before analysis. The diluted bio oil was spiked with model compounds (200 mg/kg each).

131

## 132 *2.2. UHPSFC-UV instrument and column*

133 All experiments were performed on an Acquity UPC<sup>2</sup> instrument (Waters, Milford, MA, USA).  
134 Key parameters (stationary and mobile phases, back pressure, column temperature and  
135 gradient conditions) were optimized according to a procedure developed in a previous work  
136 and based on the maximization of peak capacity [10]. The mobile phase flow-rate was 1.4  
137 mL/min. The organic solvent modifier was a mix of acetonitrile and water (98/2 v/v). The oven  
138 temperature was set at 30 °C. Back Pressure Regulator (BPR) was set at 150 bar. The injection  
139 volume was 1 µL. The column used was an Acquity BEH-2EP (100 x 3mm, 1.7µm). The mobile  
140 phase varied from 1% to 40 % of organic solvent modifier in 14 minutes. The injector needle  
141 was washed with 600 µL of methanol after each injection. The column outlet was connected  
142 to a photo-diode array detector (PDA) equipped with a 8µL high pressure UV cell (400 bars)  
143 with a path length of 10 mm. The detection wavelengths varied between 210 and 400 nm with  
144 a resolution of 1.2 nm. The sampling rate was set at 40 Hz. The instrument control was  
145 performed by Empower 3 software (Waters).

146

## 147 *2.3. HRMS instrument*

148 Mass spectra were obtained with an Ion Trap –Time of Flight (IT-ToF) instrument (Shimadzu,  
149 Kyoto, Japan) equipped with an atmospheric pressure chemical ionization (APCI) source  
150 operated in negative mode. The resolution was 9385 for m/z=520.9095. Mass error was 5 ppm  
151 with internal calibration and 20 ppm with external calibration using sodium formate clusters  
152 to enlarge the range of calibration from 45 to 928 Th. MS parameters were optimized in order  
153 to favor the detection of pseudo-molecular ions. Mass range was between 80 and 800 uma;  
154 accumulation time was set at 30 ms; nebulizing gas flow was 0.5L/min; drying gas pressure  
155 was 100 kPa, both APCI and CDL temperatures were set at 250 °C while the heat block  
156 temperature at 280 °C. . The optimization of the interface between SFC and MS is presented  
157 in the Result section.

158

## 159 *2.4. MS data processing*

160 The APCI source mode was selected for this study. Corresponding MS data represent a large  
161 amount of information and therefore require suitable data processing to achieve the  
162 identification of a maximum of compounds. Starting from raw data, the obtained

163 chromatograms with MS (total ion current) or ultra violet (UV) detection were not sufficient  
164 to get relevant information. Data were therefore represented using a 2D-colour plot (mass-  
165 map) with information on retention time (x-axis), mass over charge  $m/z$  ratio (y-axis) and  
166 intensity (color scale). Peak intensity was described by a logarithmical color gradient. However it is  
167 important to note that peak intensities should not be directly compared since ionization yields strongly  
168 depend on compound chemical structures. For each mass-map spot, there may be numerous  
169 possible structures. As a result HRMS data were processed with an in-house software (so-  
170 called SFC/MS software in the rest of the study), in order to get accurate mass measurement  
171 and hence a set of several formulae for each mass-map spot. This in-house software was  
172 developed with the objective of (i) drawing and comparing mass-maps, (ii) being as universal  
173 as possible and (iii) maintaining the whole control regarding further identification procedure.  
174 The file format is based on the widely used mzXML extension [15], allowing the use of a large  
175 range of chromatographic (LC, LCxLC, SFC) and mass spectrometry (ToF, Orbitrap, FT-  
176 ICR/MS...) systems. For molecular formula calculation, the following parameters were used:  
177 elemental composition  $^{12}\text{C}_{1-50}$ ,  $^1\text{H}_{1-100}$ ,  $^{16}\text{O}_{0-20}$ ,  $^{14}\text{N}_{0-1}$  ( $^{13}\text{C}$  were also taken into account) ; mass  
178 error inferior or equal to  $\pm 20$  ppm ; H/C ratio = 0.2-3.1, O/C ratio = 0-1.8 ; N/C ratio = 0-1.3.  
179 In case of several possible molecular formulae, the most likely one was selected so that a  
180 unique elemental composition ( $\text{C}_c\text{H}_h\text{O}_o\text{N}_n$ ) was assigned to a given  $m/z$  value. For each  
181 molecular formula, a score was calculated based on both mass error and isotopic data  
182 (equally) and the molecular formula having the highest score was selected. In addition, due to  
183 the fact that the elution of a given compound can take a few seconds, the corresponding data  
184 were lumped together which could avoid the risk of double identification. To validate the  
185 identification procedure, a mixture of 36 model compounds (Table S1 of the supplementary  
186 information) was analyzed alone and spiked in a bio-oil in order to point out possible matrix  
187 effects which could hinder the identification procedure. The concentration of each compound  
188 was 200 mg/kg in tetrahydrofuran (THF). The objective was to find, in both cases, the correct  
189 molecular formula for each model compound.

190

## 191 *2.5. FT-ICR/MS instrument*

192 The FT-ICR/MS instrument used for comparison with SFC-HRMS analysis was a Thermo  
193 Scientific LTQ FT Ultra (Bremen, Germany) composed of a linear ion trap and an ioncyclotron  
194 resonance cell in a 7 Tesla superconducting magnet. Sample was diluted in methanol (1:50 ;

195 v:v) prior to the injection by infusion mode (5 $\mu$ L/min) and ionized by APCI mode. The number  
196 of microscans were set at 8 and 50 scans were accumulated. Data treatment was achieved  
197 with an in-house software called KendrickInside. For molecular formula calculation, the  
198 following parameters were used: elemental composition  $^{12}\text{C}_{1-50}$ ,  $^1\text{H}_{1-100}$ ,  $^{16}\text{O}_{0-20}$ ,  $^{14}\text{N}_{0-1}$  ( $^{13}\text{C}$  were  
199 also taken into account) ; mass error lower or equal to + 5 ppm.

200

201

### 202 3. RESULTS AND DISCUSSION

203

#### 204 3.1. Optimization of SFC(-)APCI-HRMS interface

205 With an APCI ionization source as used in this study, the mobile phase is under atmospheric  
206 pressure when entering the source, which results in  $\text{CO}_2$  decompression in the introduction  
207 capillary. The resulting  $\text{CO}_2$  evaporation makes the compounds concentrated in the liquid  
208 solvent (co-solvent). There may be therefore a risk of sample precipitation in the capillary,  
209 especially when the concentration of organic modifier in the mobile phase is low, for instance  
210 in starting gradient conditions. To prevent this from occurring, an additional pump can be used  
211 to deliver an additional amount of liquid solvent. Such device (so called Isocratic Solvent  
212 Manager – ISM), as proposed by Waters for our UHPSFC instrument, enables to add the  $\text{CO}_2$ -  
213 miscible make-up solvent (i.e. methanol) to the mobile phase via a T-union. Fig.1 shows the  
214 interface configuration (delimited by a frame) which also includes a second zero-dead volume  
215 T-union designed to split the flow coming from the first T-union in such a way that a fraction  
216 of the total flow is directed towards BPR device and the other one towards MS. Adding a protic  
217 solvent is also intended to improve the ionization yield by promoting charge exchange.  
218 However, with such interface configuration and the present APCI-IT-ToF-MS instrument, the  
219 MS signal was not stable enough, suggesting that the amount of solvent entering the APCI  
220 source was too low. A second make-up pump had therefore to be added along with a third  
221 zero-dead volume T-union to increase the flow-rate entering the APCI source as further  
222 discussed. The following discussion presents a theoretical approach to explain the limitation  
223 encountered with the commercially available interface and the procedure we used to optimize  
224 the second make-up conditions (flow-rate and solvent composition).

225 The solvent flow-rate entering the ionization source should be adapted according to the  
226 ionization source specificity. That requires that its value could be reliably predicted, depending

227 on SFC parameters and interface conditions. Theoretically, it is possible to predict the solvent  
228 flow-rate, knowing the pressure drop in the tubing, the flow-rates delivered by both SFC pump  
229 and ISM, the tubing geometry and the concentration of organic solvent in the mobile phase.  
230 According to the Poiseuille-Hagen law, the pressure drop in the tubing is given by

231 
$$\Delta P = \frac{128 \eta}{\pi} \times R \times F \quad (1)$$

232 Where  $F$ , is the flow-rate through the tubing,  $R$ , a term taking into account the tubing  
 233 dimensions ( $R = L/d^4$ ,  $L$  and  $d$  being the tubing length and diameter respectively) and  $\eta$ , the  
 234 viscosity of the fluid (i.e. the fluid composed of CO<sub>2</sub> and organic solvents coming from both  
 235 SFC and make-up pumps).

236 The total flow-rate,  $F_T$ , prior to the second T-union is given by

$$237 \quad F_T = F_{MS} + F_W \quad (2)$$

238 where,  $F_{MS}$  and  $F_W$  are the flow-rates after the splitter, towards MS and the waste.  $F_T$  is also  
 239 given by the sum of flow-rates entering the first T-union:

$$240 \quad F_T = F_{SFC} + F_{Pump\ 1} \quad (3)$$

241 where,  $F_{SFC}$  and  $F_{pump\ 1}$  are the flow-rates delivered by SFC pump and Pump #1 respectively.

242 As shown in Fig 1, the section between the second T-union and the ionization source, is  
 243 composed of two different tubes (blue and red in Fig.1) connected by a zero dead volume  
 244 union. The red one diameter being significantly larger than the blue one (175 $\mu$ m vs 50 $\mu$ m),  
 245 the pressure drop involved may not be considered in the calculations. Considering the same  
 246 pressure drop in the two paths located after the splitter (second T-union),  $F_{MS}$  can be  
 247 calculated according to

$$248 \quad F_{MS} = \frac{\frac{\Delta P_{BPR} \times \pi}{128 \eta} + R_W \times F_T}{(R_W + R_{MS})} \quad (4)$$

249  $\Delta P_{BPR}$  is the back pressure due to BPR.  $R_W$  and  $R_{MS}$  (Eq.1) relate to the capillaries located  
 250 between the second T-union and BPR and between the second T-union and MS inlet  
 251 respectively (the pressure drop in the tube located between the third T-union and MS inlet  
 252 was low enough to be not taken into account).

253 The fraction,  $X_s$ , of solvent after the first T-union is given by

$$254 \quad X_s = \frac{X_{s,SFC} \times F_{SFC} + F_{Pump\ 1}}{F_T} \quad (5)$$

255 where  $X_{s,SFC}$  is the volume fraction of solvent in SFC mobile phase. Finally, by combining Eqs. 4  
 256 and 5, the predicted solvent flow-rate entering the MS source can be calculated according to

$$257 \quad F_{S,MS} = \frac{X_{s,SFC} \times F_{SFC} + F_{pump\ 1}}{F_T} \times \frac{\frac{\Delta P_{BPR} \times \pi}{128 \eta} + R_W \times F_T}{(R_W + R_{MS})} + F_{Pump\ 2} \quad (6)$$

258 With  $F_{Pump\ 2}$  being the solvent flow-rate delivered by Pump #2 (Fig.1). Eq.6 can be considered  
 259 as valid provided that (i) the fluid viscosity can be accurately assessed, (ii) the fluid viscosity is  
 260 constant along the tube located between the second and the third T-union in spite of CO<sub>2</sub>

261 decompression; (iii) the tubing dimensions are reliable and (iv) the solvent fraction,  $X_s$ , is  
262 maintained after flow-splitting. Flow-rate predictions can be inaccurate if one or more of these  
263 conditions are not fulfilled. We therefore compared some experimental measures to the  
264 predicted values given by Eq.6 in order to assess the validity of this theoretical approach. The  
265 measures were carried out without Pump 2 ( $F_{\text{Pump } 2} = 0$ ) with acetonitrile (ACN) as co-solvent  
266 and methanol as make-up solvent. The make-up flow was varied from 200 to 1500  $\mu\text{L}/\text{min}$ .  
267 SFC mobile phase conditions were those optimized in a previous study [10] and described in  
268 the experimental section. Two different co-solvent concentrations were considered,  
269 corresponding to initial and final gradient compositions (i.e. 1% ACN and 40% ACN). Flow-rate  
270 measurements were performed according to a method previously described [16]. Fluid  
271 viscosity values were estimated based on experimental correlations proposed by Ouyang [17],  
272 recently applied to SFC-MS with methanol as co-solvent [16] and adapted to binary mixtures  
273 of acetonitrile and methanol. As illustrated in Fig.2, showing the variation of solvent flow  
274 entering MS with Pump #1 flow, experimental and predicted values are in very good  
275 agreement for the two studied co-solvent compositions (i.e. 1% ACN and 40% ACN), thereby  
276 validating our theoretical approach. Fig.2 also shows that an increase in the make-up flow  
277 (containing MeOH) or in ACN concentration in SFC mobile phase, increases the solvent flow-  
278 rate entering the ionization source. However both curves tend towards the same constant  
279 value of nearly 300  $\mu\text{L}/\text{min}$  which was found to be the threshold value to get a stable signal  
280 with the APCI source. The first option to increase the solvent flow could be to change the  
281 restriction capillary dimensions (red one in Fig.1). As theoretically shown in Fig. 3a for a mobile  
282 phase composition of 1% ACN, a reduction of the capillary length from 75 to 45 cm should  
283 lead to an increase in solvent flow from 230  $\mu\text{L}/\text{min}$  to 380  $\mu\text{L}/\text{min}$ , for a make-up flow of 500  
284  $\mu\text{L}/\text{min}$ . Meanwhile, the split ratio increases from 0.45 to 0.72 as illustrated in Fig. 3b. For a  
285 given capillary length, Fig.3 clearly shows that increasing the make-up flow slightly increases  
286 the solvent flow entering MS but strongly decreases the split ratio and hence the signal  
287 intensity in case of mass flow dependent detectors such as APCI-MS as also discussed  
288 elsewhere [18]. In summary, the first option could be the use of a restriction capillary with 45  
289 cm length (instead of 75 cm proposed in the commercial interface) at a make-up flow of  
290 500 $\mu\text{L}/\text{min}$ .

291 The second option considered in the present study involved no change in the commercially  
292 available interface but the addition of a second make-up solvent prior to MS inlet (Pump #2).

293 The advantage of this second option lies in the fact that optimizing, for this second make-up,  
294 both solvent flow-rate and solvent composition, should provide more versatile solutions  
295 depending on the type of complex sample and also depending on the polarity of APCI  
296 ionization source. The selection of the type of solvent entering APCI source may be of first  
297 importance to make easier the charge exchange between analytes and nitrogen plasma  
298 around the Corona needle. Water is usually recommended as additional solvent to enhance  
299 the ionization yield with an APCI source. Accordingly, a mixture of water and MeOH was  
300 considered within a composition range between 35/65 and 65/35 (water/MeOH, V/V). The  
301 solvent flow-rate was studied in the range 100-300  $\mu\text{L}/\text{min}$ . Both ranges were found to be  
302 suitable in terms of both signal intensity and signal stability from a preliminary study with 15  
303 model compounds detected in (-)APCI/HRMS (see Table 1). Model compounds were selected  
304 according to published studies on bio oil matrices and so that their retention times covered  
305 the whole retention space. 9 experiments well distributed among the parameter space were  
306 carried out with the proposed commercial interface at a make-up #1 flow of 500 $\mu\text{L}/\text{min}$ . For  
307 each of the 15 compounds, the signal-to-noise ratio, obtained with a given set of conditions  
308 was normalized with respect to the 9 sets of conditions, thereby providing a radar plot and a  
309 corresponding delimited area as shown in Fig. 4a. The calculated response function  
310 represented the fraction of the space occupied by the colored area and therefore varied  
311 between 0 and 1. The response function was fitted with a polynomial function. The resulting  
312 response surface in Fig.4b shows that the highest response values correspond to low flow-  
313 rates and high water concentrations. The response surface is curved with minimum response  
314 values at intermediate solvent compositions (i.e. around 50% water) which supports the  
315 necessity to optimize. It is important to note that optimization results are expected to be fully  
316 dependent on the analytes and it is therefore essential to carefully choose model compounds  
317 in accordance with the studied complex matrix and, if possible, with their retention times well  
318 distributed among the separation space as done in the present study.

319 Finally, our optimized conditions consisted in keeping the proposed commercial interface with  
320 a make-up solvent #1 composed of methanol at a flow-rate of 500  $\mu\text{L}/\text{min}$  and a make-up  
321 solvent #2 composed of 65% water and 35% MeOH at a flow-rate of 100 $\mu\text{L}/\text{min}$ .

322

323 *3.1. SFC-(-)APCI/HRMS results for model compounds*

324 The analysis of complex samples such as biomass fast pyrolysis bio-oils by SFC-HRMS  
325 generates a huge amount of data that are not easy to process without dedicated software.  
326 We therefore built our own SFC/MS software as described in Materials and methods Section.  
327 This software was designed to attribute a molecular formula to each mass peak detected  
328 during the SFC run. The applied procedure was carried out according to the following golden  
329 rules suggested by Kind et al. [19] for filtering molecular formulae obtained by accurate mass  
330 spectrometry: (i) use any information about the sample (e.g. the major elements present and  
331 their relative abundance); (ii) use isotopic distribution around pseudo molecular ion signal;  
332 (iii) limit the number of heteroatoms in the molecular formula; (iv) use the ratios H/C and  
333 heteroatom/C to reduce the number of possibilities. The SFC/MS software was challenged  
334 with the SFC(-)APCI/HRMS analysis of a mixture containing 36 model compounds (see Table  
335 S1 in Supplementary Information), first dissolved in THF and then spiked in a bio-oil sample in  
336 order to highlight possible matrix effects which could reduce the ionization yield and hence  
337 could alter the quality of information. The results are displayed in Figs. 5a and 5b respectively,  
338 with base peak chromatogram (BPC) at the bottom and mass map at the top. For model  
339 compounds alone (Fig.5a), 15 peaks can be observed, well distributed across the separation.  
340 However 19 peaks were detected in (-)APCI/HRMS, suggesting that some model compounds  
341 were not separated in SFC (i.e peaks #2, #3 and #4; #5 and #6; #8 and #9 as can be seen in  
342 Fig.5b). The mass map generated by SFC/MS software allowed to add a third dimension  
343 corresponding to the mass over charge ratio ( $m/z$ ). From these data, a unique molecular  
344 formula was proposed for each of the 19 detected compounds. Compound names, retention  
345 times, measured masses, molecular formulae resulting from SFC/MS calculation and  
346 corresponding mass errors are listed in Table 1. It is interesting to notice that, for each  
347 detected molecule, the accurate mass measurement allowed to propose the expected  
348 molecular formula, thereby leading to unambiguous molecular identification. For the sample  
349 composed of model compounds spiked in the bio-oil, the same 19 molecules could be  
350 detected and their molecular formulae identified in spite of possible matrix effects due to the  
351 presence of a very large number of components in bio-oil samples. By showing no effect of  
352 the bio-oil matrix on the ionization yield, these results ensure the suitability of the proposed  
353 method for formula identification.

354

355

### 3.2. SFC(-)APCI/HRMS results for a biomass fast pyrolysis oil

356 Similarly, a bio-oil was analyzed with the same optimized conditions, using the same  
357 procedure. The results in terms of BPC chromatogram and mass map are shown in Fig.5c.

358 These results give some valuable insights:

359 (i) The mass range ( $m/z$ ) seems to be mainly between 150 and 400 uma which points out the  
360 complementarity of SFC and GCxGC which is known to provide a mass range rather between  
361 0 and 200 uma [6].

362 (ii) The separation space is well occupied by the components except in the first part of the  
363 chromatogram corresponding to the isocratic step. This is not supported by UV detection  
364 which allowed to observe a large number of peaks in this first part [10] (see Fig. S1 in  
365 supplementary Information). Such peaks detected in UV but not detected in (-)APCI  
366 correspond to components, such as furans or non-aromatic ketones that are not easily ionized  
367 in APCI source. A complementary analysis with positive ionization could bring additional  
368 information on compounds that are more prone to favor the formation of  $[M + H]^+$  ions.

369 (iii) From MS spectra resulting from SFC(-)APCI/HRMS bio-oil analysis, 1379 molecular  
370 formulae could be proposed by our LC/SFC software. Among them, those corresponding to a  
371 model compound detected were investigated and 12 molecular formulae were found. They  
372 are listed in Table 2 along with their corresponding information (mass errors, retention times  
373 of both model compounds and similar molecular formulae found in the bio-oil). The difference  
374 in retention times (Table 2) allowed us to assess the degree of fit that the bio-oil compound  
375 had relative to the model compound. Based on a difference lower than 0.1 min, 7 model  
376 compounds (numbered in Table 1) or their positional isomers were strongly suspected to be  
377 present in the studied bio-oil: isoeugenol (#4), methoxynaphtol (#6), vanillin (#7),  
378 coniferaldehyde (#8), catechol (#12), vanillic acid (#16) and sinapic acid (#19). Moreover 5  
379 model compounds that could be detected either alone or spiked in the bio-oil could not be  
380 detected in the bio-oil at their expected retention times. However their molecular formulae  
381 were identified at retention times significantly different, suggesting the presence of structural  
382 isomers.

383 (iv) Such mass maps could be easily used as characteristic fingerprints of complex samples  
384 allowing for in depth comparison of different samples.

385 The presence of different structural and/or positional isomers in the bio-oil was confirmed by  
386 a list of molecular formulae (Table 3) that were identified at different retention times. This  
387 result supports the fact that SFC can be a powerful analytical tool to discriminate compounds

388 having the same molecular formulae but different retention times, which is not possible with  
389 any direct HRMS analysis in direct infusion mode (i.e. without prior separation).

390 The heteroatom class distribution, with oxygen families ranging from O<sub>1</sub> to O<sub>15</sub> and nitrogen  
391 family O<sub>x</sub>N<sub>1</sub>, is presented in Fig.6 for three equal parts of the SFC separation. Such data  
392 representation is often used with HRMS analysis. As can be observed and already highlighted,  
393 very few components could be detected in the first part of the separation. Although relative  
394 abundance distributions strongly depend on ionization conditions as well as on bio-oil  
395 properties, it can be observed that O<sub>11</sub> to O<sub>15</sub> families (most oxygenated compounds) were  
396 mainly detected in the third part while O<sub>2</sub> to O<sub>6</sub> families were more intense in the second part  
397 which is consistent with expected retention in SFC on a polar stationary phase (i.e. Acquity  
398 BEH-EP)

399

### 400 3.1. Comparison of SFC-HRMS and FT-ICR/MS analysis of a biomass fast pyrolysis oil

401 In order to have a clear idea about how the proposed analytical technique can be  
402 complementary to modern HRMS techniques offering very high resolving power, we  
403 compared SFC-HRMS to FT-ICR/MS (Fourier transform-ion cyclotron resonance mass  
404 spectrometry) for the specific case of bio-oil analysis. Since several years, HRMS techniques  
405 alone are being increasingly used to describe the composition of biomass fast pyrolysis oils  
406 [3]. In particular, FT-ICR/MS has gained in interest over the past ten years, providing key  
407 information in terms of m/z ratios, molecular formulae and double bond equivalent (DBE)  
408 for compounds being detected essentially by electrospray ionization source, and more  
409 scarcely by APPI [20–25]. In this work, the studied bio-oil was also analyzed by FT-ICR/MS using  
410 an APCI source in negative mode and the resulting data were compared with those obtained  
411 in SFC(-)APCI/HRMS. A very large number of peaks (i.e. 3949 identified molecular formulae)  
412 were detected by FT-ICR/MS, illustrating its huge sensitivity compared to SFC-IT-TOF/MS (i.e.  
413 1379 identified molecular formulae). However it is interesting to notice that among all the  
414 molecular formulae identified by FT-ICR/MS and SFC/MS, only 835 were common to both  
415 techniques. That underlines the great benefit of SFC prior to HRMS which enables the  
416 separation of several positional or structural isomers (as shown in Table 3) while direct  
417 injection in FT-ICR/MS cannot differentiate them, leading to the same molecular formula if no  
418 additional structural data are provided.

419 It should be noted that, similarly to SFC-HRMS, the results obtained in FT-ICR/MS must only  
420 be used for qualitative analysis due to the dependence of the response factor on the  
421 compound. This also implies that any attempt to compare FT-ICR/MS and SFC-HRMS data  
422 must be done with caution. However the heteroatom class distributions might be compared  
423 in terms of their relative abundance. It appears in Fig.7 that both distributions are different  
424 although the ionization source (i.e. (-)APCI) was the same. Our (-)APCI/FT-ICR/MS results are  
425 quite consistent with reported studies dealing with (-)ESI/FT-ICR/MS in which distributions  
426 were focused on O<sub>3</sub> to O<sub>8</sub> families [22,26–28]. The comparison of both heteroatom class  
427 distributions (Fig.7) indicates that same ranges of O<sub>x</sub> families are covered by FT-ICR/MS and  
428 SFC-HRMS, with a clear benefit of SFC-HRMS to specifically analyze molecules having low  
429 number of oxygen atoms (O<sub>1</sub>-O<sub>3</sub>), suggesting that SFC separation prior to HRMS detection  
430 greatly enhances the detection of such species by preventing from strong ion suppression  
431 which may occur when the whole bio-oil is directly introduced in FT-ICR/MS. Indeed some  
432 reported studies on different biomass products have proved that polar analytes are much more  
433 affected by matrix effects than nonpolar ones [29,30]. Furthermore the relative intensity for O<sub>12</sub>  
434 to O<sub>15</sub> families seems to be higher in SFC-HRMS than in FT-ICR. These results also suggest that  
435 a better ionization yield can be achieved in SFC-HRMS for these highly-oxygenated  
436 compounds, thereby still supporting the fact that the separation prior to HRMS can be very  
437 useful.

438 Another interesting way to present the results and to get relevant information about bio-oil  
439 composition consists in drawing van Krevelen diagram, based upon elemental formulae, in the  
440 form of a dot matrix representing H/C ratio versus O/C ratio (Fig.8). These ratios are  
441 characteristic of a compound class which can be identified by a delimited area in the diagram.  
442 As underlined by Stas et al. [3], this diagram can be used to evaluate (1) the abundance of  
443 compounds from different classes and (2) the correlation between compounds from different  
444 classes. Both van Krevelen diagrams derived from SFC-(-)APCI/MS (Fig. 8a) and FT-ICR/MS  
445 (Fig. 8b) data are in good agreement. Detected species are intensively focused within areas  
446 usually dedicated to phenolics (i.e. O/C = 0-0.6; H/C = 0.5-1.5) and carbohydrates (i.e. O/C =  
447 0.6-1.1 ; H/C > 1.5). This shows that a high number of compounds exhibiting a medium polarity  
448 are present in the studied bio-oil and can be detected by (-) APCI.

449

#### 450 **4. Conclusion**

451 This study presents the first detailed characterization of a bio-oil by SFC hyphenated to HRMS  
452 with negative ion APCI as ionization source. The interface between SFC and (-)APCI/HRMS was  
453 optimized for a specific commercial equipment with a procedure that can be applied in the  
454 future to any ionization source and any commercially available equipment provided that  
455 tubing geometry are known and model compounds are available.

456 As shown, this coupling can be a valuable technique for assessing bio-oil composition and an  
457 alternative and complement to more usual methods such as HRMS alone or GCxGC-MS. It was  
458 pointed out that some model compounds could not be detected by using the single negative  
459 ion APCI as ionization technique, suggesting that additional ionization techniques (i.e. APCI in  
460 positive mode and ESI in positive and negative modes) should be combined to achieve a more  
461 comprehensive bio-oil analysis.

462 In spite of very attractive analytical possibilities due to its very high resolving power, FT-  
463 ICR/MS alone cannot permit the distinction between positional and structural isomers which  
464 can be abundant in complex samples such as bio-oils as highlighted in this study. Moreover, a  
465 clear reduction of signal intensity, likely due to matrix effects, was pointed out in FT-ICR/MS.  
466 Overall, SFC-HRMS is a very promising analytical tool for the analysis of complex chemical  
467 samples. The proposed mass-maps as characteristic fingerprints could be useful for in-depth  
468 comparison of complex samples. Finally, considering the ability of SFC to both separate  
469 isomers and reduce matrix effects, its hyphenation to high resolution mass spectrometry can  
470 provide an access to a large number of detailed data, mandatory to go further on complex  
471 sample characterization.

472

473

#### 474 **References**

475

- 476 [1] A.V. Bridgwater, H. Hofbauer, S. van Loo, Thermal Biomass Conversion, 2009.  
477 [2] C.M. Michailof, K.G. Kalogiannis, T. Sfetsas, D.T. Patiaka, A.A. Lappas, Advanced analytical  
478 techniques for bio-oil characterization, WIREs Energy Environ 5 (6) (2016) 614–639.  
479 [3] M. Staš, J. Chudoba, D. Kubička, J. Blažek, M. Pospíšil, Petroleomic Characterization of  
480 Pyrolysis Bio-oils: A Review, Energy Fuels 31 (10) (2017) 10283–10299.

- 481 [4] P.K. Kanaujia, Y.K. Sharma, U.C. Agrawal, M.O. Garg, Analytical approaches to  
482 characterizing pyrolysis oil from biomass, *TrAC Trends in Analytical Chemistry* 42 (2013)  
483 125–136.
- 484 [5] N. Charon, J. Ponthus, D. Espinat, F. Broust, G. Volle, J. Valette, D. Meier, Multi-technique  
485 characterization of fast pyrolysis oils, *Journal of Analytical and Applied Pyrolysis* 116  
486 (2015) 18–26.
- 487 [6] M. Stas, D. Kubic, J. Chudoba, M. Pospíš, Overview of Analytical Methods Used for  
488 Chemical Characterization of Pyrolysis Bio-oil, *Energy Fuels* (28) (2014) 385–402.
- 489 [7] A. Le Masle, D. Angot, C. Gouin, A. D'Attoma, J. Ponthus, A. Quignard, S. Heinisch,  
490 Development of on-line comprehensive two-dimensional liquid chromatography method  
491 for the separation of biomass compounds, *Journal of chromatography A* 1340 (2014) 90–  
492 98.
- 493 [8] D. Tomasini, F. Cacciola, F. Rigano, D. Sciarrone, P. Donato, M. Beccaria, E.B. Caramão, P.  
494 Dugo, L. Mondello, Complementary Analytical Liquid Chromatography Methods for the  
495 Characterization of Aqueous Phase from Pyrolysis of Lignocellulosic Biomasses, *Anal.*  
496 *Chem.* 86 (22) (2014) 11255–11262.
- 497 [9] M. Sarrut, A. Corgier, G. Crétier, A. Le Masle, S. Dubant, S. Heinisch, Potential and  
498 limitations of on-line comprehensive reversed phase liquid chromatography×supercritical  
499 fluid chromatography for the separation of neutral compounds: An approach to separate  
500 an aqueous extract of bio-oil, *Journal of chromatography A* 1402 (2015) 124–133.
- 501 [10] J. Crepier, A. Le Masle, N. Charon, F. Albrieux, S. Heinisch, Development of a supercritical  
502 fluid chromatography method with ultraviolet and mass spectrometry detection for the  
503 characterization of biomass fast pyrolysis bio oils, *Journal of Chromatography A* 1510  
504 (2017) 73-81.
- 505 [11] E. Lemasson, S. Bertin, P. Hennig, E. Lesellier, C. West, Comparison of ultra-high  
506 performance methods in liquid and supercritical fluid chromatography coupled to  
507 electrospray ionization - mass spectrometry for impurity profiling of drug candidates,  
508 *Journal of chromatography A* 1472 (2016) 117–128.
- 509 [12] L. Novakova, M. Rentsch, A. Grand-Guillaume Perrenoud, R. Nicoli, M. Saugy, J.-L.  
510 Veuthey, D. Guillarme, Ultra high performance supercritical fluid chromatography  
511 coupled with tandem mass spectrometry for screening of doping agents. II: Analysis of  
512 biological samples, *Analytica Chimica Acta* 853 (2015) 647–659.

- 513 [13] D. Spaggiari, F. Mehl, V. Desfontaine, A. Grand-Guillaume Perrenoud, S. Fekete, S. Rudaz,  
514 D. Guillarme, Comparison of liquid chromatography and supercritical fluid  
515 chromatography coupled to compact single quadrupole mass spectrometer for targeted  
516 in vitro metabolism assay, *Journal of chromatography A* 1371 (2014) 244–256.
- 517 [14] J. Duval, C. Colas, V. Pecher, M. Poujol, J.-F. Tranchant, E. Lesellier, Hyphenation of ultra  
518 high performance supercritical fluid chromatography with atmospheric pressure  
519 chemical ionisation high resolution mass spectrometry: Part 1. Study of the coupling  
520 parameters for the analysis of natural non-polar compounds, *Journal of chromatography*  
521 *A* 1509 (2017) 132–140.
- 522 [15] P.G.A. Pedrioli, J.K. Eng, R. Hubley, M. Vogelzang, E.W. Deutsch, B. Raught, B. Pratt, E.  
523 Nilsson, R.H. Angeletti, R. Apweiler, K. Cheung, C.E. Costello, H. Hermjakob, S. Huang, R.K.  
524 Julian, E. Kapp, M.E. McComb, S.G. Oliver, G. Omenn, N.W. Paton, R. Simpson, R. Smith,  
525 C.F. Taylor, W. Zhu, R. Aebersold, A common open representation of mass spectrometry  
526 data and its application to proteomics research, *Nature biotechnology* 22 (11) (2004)  
527 1459–1466.
- 528 [16] A. Grand-Guillaume Perrenoud, C. Hamman, M. Goel, J.-L. Veuthey, D. Guillarme, S.  
529 Fekete, Maximizing kinetic performance in supercritical fluid chromatography using  
530 state-of-the-art instruments, *Journal of chromatography A* 1314 (2013) 288–297.
- 531 [17] L.-B. Ouyang, New Correlations for Predicting the Density and Viscosity of Supercritical  
532 Carbon Dioxide Under Conditions Expected in Carbon Capture and Sequestration  
533 Operations, *TOPEJ* 5 (1) (2011) 13–21.
- 534 [18] D. Guillarme, V. Desfontaine, S. Heinisch, J.-L. Veuthey, *Journal of Chromatography B*  
535 (2018) Submitted.
- 536 [19] T. Kind, O. Fiehn, Seven Golden Rules for heuristic filtering of molecular formulas  
537 obtained by accurate mass spectrometry, *BMC bioinformatics* 8 (2007) 105.
- 538 [20] N.S. Tessarolo, R.V.S. Silva, G. Vanini, A. Casilli, V.L. Ximenes, F.L. Mendes, A. Rezende  
539 Pinho, W. Romão, E.V.R. Castro, C.R. Kaiser, D.A. Azevedo, Characterization of thermal  
540 and catalytic pyrolysis bio-oils by high-resolution techniques: <sup>1</sup>H NMR, GC × GC-TOFMS  
541 and FT-ICR MS, *Journal of Analytical and Applied Pyrolysis* 117 (2016) 257–267.
- 542 [21] N.S. Tessarolo, R.C. Silva, G. Vanini, A. Pinho, W. Romão, E.V.R. Castro, D.A. Azevedo,  
543 Assessing the chemical composition of bio-oils using FT-ICR mass spectrometry and

544 comprehensive two-dimensional gas chromatography with time-of-flight mass  
545 spectrometry, *Microchemical Journal* 117 (2014) 68–76.

546 [22] E.A. Smith, S. Park, A.T. Klein, Y.J. Lee, Bio-oil Analysis Using Negative Electrospray  
547 Ionization: Comparative Study of High-Resolution Mass Spectrometers and Phenolic  
548 versus Sugarcane Components, *Energy Fuels* 26 (6) (2012) 3796–3802.

549 [23] J.M. Jarvis, A.M. McKenna, R.N. Hilten, K.C. Das, R.P. Rodgers, A.G. Marshall,  
550 Characterization of Pine Pellet and Peanut Hull Pyrolysis Bio-oils by Negative-Ion  
551 Electrospray Ionization Fourier Transform Ion Cyclotron Resonance Mass Spectrometry,  
552 *Energy Fuels* 26 (6) (2012) 3810–3815.

553 [24] J.M. Jarvis, D.S. Page-Dumroese, N.M. Anderson, Y. Corilo, R.P. Rodgers, Characterization  
554 of Fast Pyrolysis Products Generated from Several Western USA Woody Species, *Energy  
555 Fuels* 28 (10) (2014) 6438–6446.

556 [25] I. Miettinen, M. Mäkinen, T. Vilppu, J. Jänis, Characterization of Phase-Separated Pine  
557 Wood Slow Pyrolysis Oil by Negative-Ion Electrospray Ionization Fourier Transform Ion  
558 Cyclotron Resonance Mass, *Energy Fuels* (2015).

559 [26] N. Sudasinghe, J.R. Cort, R. Hallen, M. Olarte, A. Schmidt, T. Schaub, Hydrothermal  
560 liquefaction oil and hydrotreated product from pine feedstock characterized by  
561 heteronuclear two-dimensional NMR spectroscopy and FT-ICR mass spectrometry, *Fuel*  
562 137 (2014) 60–69.

563 [27] P.V. Abdelnur, B.G. Vaz, J.D. Rocha, M.B.B. de Almeida, M.A.G. Teixeira, R.C.L. Pereira,  
564 Characterization of Bio-oils from Different Pyrolysis Process Steps and Biomass Using  
565 High-Resolution Mass Spectrometry, *Energy Fuels* 27 (11) (2013) 6646–6654.

566 [28] I. Miettinen, S. Kuittinen, V. Paasikallio, M. Mäkinen, A. Pappinen, J. Jänis,  
567 Characterization of fast pyrolysis oil from short-rotation willow by high-resolution Fourier  
568 transform ion cyclotron resonance mass spectrometry, *Fuel* 207 (2017) 189–197.

569 [29] R. Bonfiglio, R.C. King, T.V. Olah, K. Merkle, The effects of sample preparation methods  
570 on the variability of the electrospray ionization response for model drug compounds,  
571 *Rapid Communications in Mass Spectrometry* 13 (12) (1999) 1175–1185.

572 [30] Lekh Nath Sharma, Identification and Quantitation of Potential Fermentation Inhibitors  
573 in Biomass Pretreatment Hydrolysates Using High Performance Liquid Chromatography  
574 in Combination with Ultraviolet Detection and Tandem Mass Spectrometry.

575

576

577 **Figure captions**

578 Figure 1 : Schematic representation of the interface used for hyphenation of SFC to APCI/IT-  
579 TOF/MS. The proposed commercial interface is delimited by the dotted frame. T1, T2 and T3  
580 represent the 3 zero-dead volume T-unions.

581

582 Figure 2 : Variation of solvent flow entering MS source as a function of Pump #1 flow-rate for  
583 two different ACN compositions in the mobile phase (1%ACN and 40%ACN). Theoretical and  
584 experimental curves are represented by solid and dotted lines respectively. Conditions :  
585 Waters interface (see Fig.2); mobile phase flow-rate : 1.4mL/min; BPR 150 bar; 30°C.

586

587 Figure 3 : Theoretical variation of (a) solvent flow entering MS source and (b) split ratio, as a  
588 function of both Pump #1 flow-rate and restriction capillary length (i.d. 50 $\mu$ m) with 1%ACN as  
589 co-solvent. Same other conditions as in Fig.2

590

591 Figure 4 : Illustration of the response function calculation and its variation depending on  
592 solvent make-up #2 conditions. (a) Radar plots representing the normalized signal-to-noise  
593 ratio for 15 model compounds (see Table 1 for the numbering) obtained with a given set of  
594 conditions. The response function is the fraction of the space occupied by the blue colored  
595 area (b) Response function versus both the Pump #2 flow and the composition of solvent.

596

597 Figure 5 : Mass maps and Base Peak Chromatograms of (a) model mix; (b) spiked bio-oil sample  
598 and (c) bio-oil sample analyzed in SFC(-)APCI/HRMS. Detected model compounds are  
599 numbered in the different figures. (see Table 1 for analytical results) . Chromatographic  
600 conditions are given in Materials and methods Section.

601

602 Figure 6 : Heteroatom class distributions for the first (blue), second (red) and third part (green)  
603 of the SFC separation derived from (-) APCI/HRMS mass spectra. Sample: fast pyrolysis bio-oil.  
604 SFC and MS conditions given in Materials and methods Section.

605

606 Figure 7 : Comparison of heteroatom class distributions between SFC-(-)APCI/HRMS and FT-  
607 ICR/MS, both with negative ion APCI as ionization source. Conditions given in Materials and  
608 methods Section.

609

610 Figure 8 : Comparison of the van Krevelen diagrams (H/C vs O/C) of a bio-oil, obtained from  
611 (a) (-)APCI/FT-ICR/MS and (b) SFC-(-)APCI/HRMS data. Each dot corresponds to an identified  
612 molecular formula with color related to its relative abundance. Fast pyrolysis bio-oil sample.  
613 SFC and MS conditions given in Materials and methods Section.

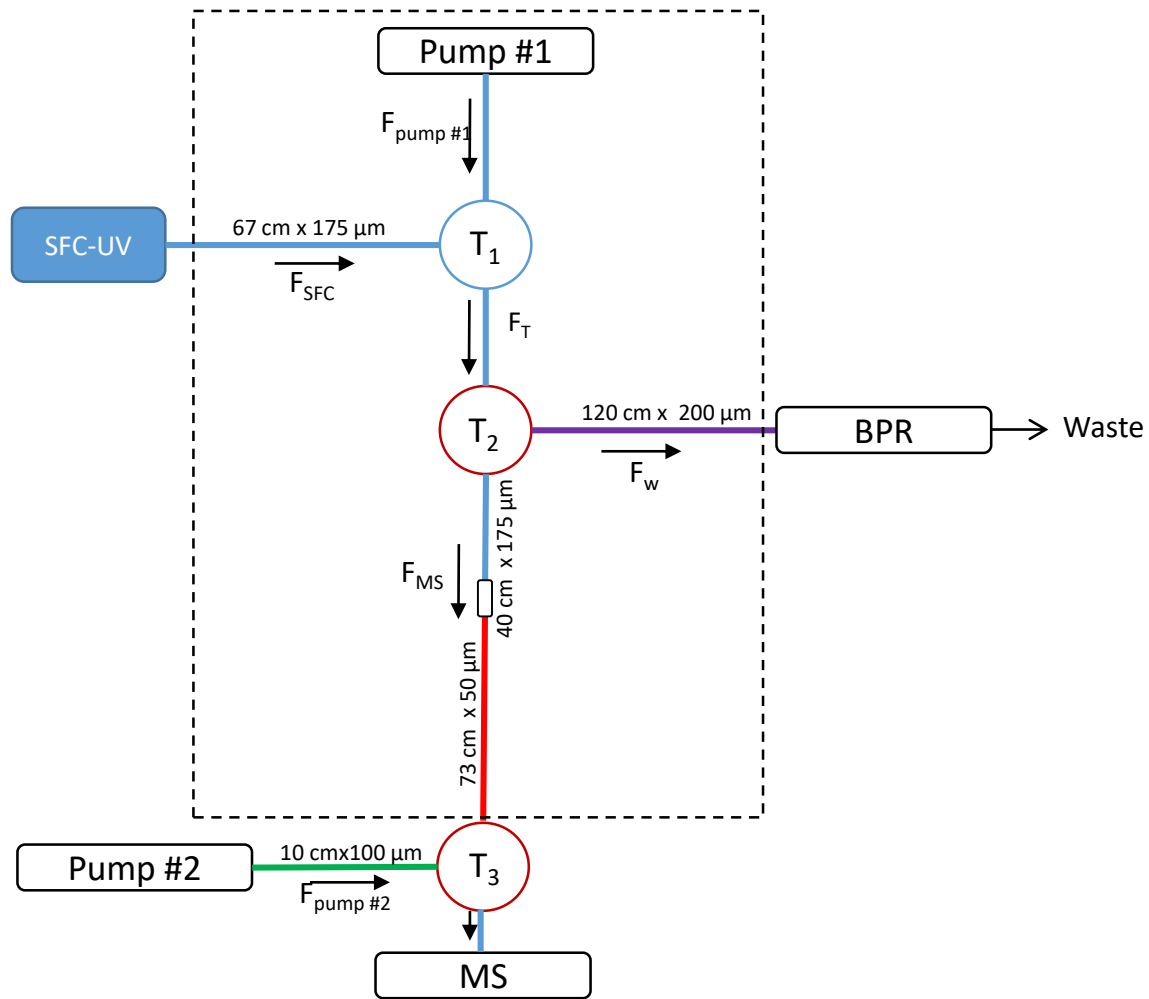


Figure 1

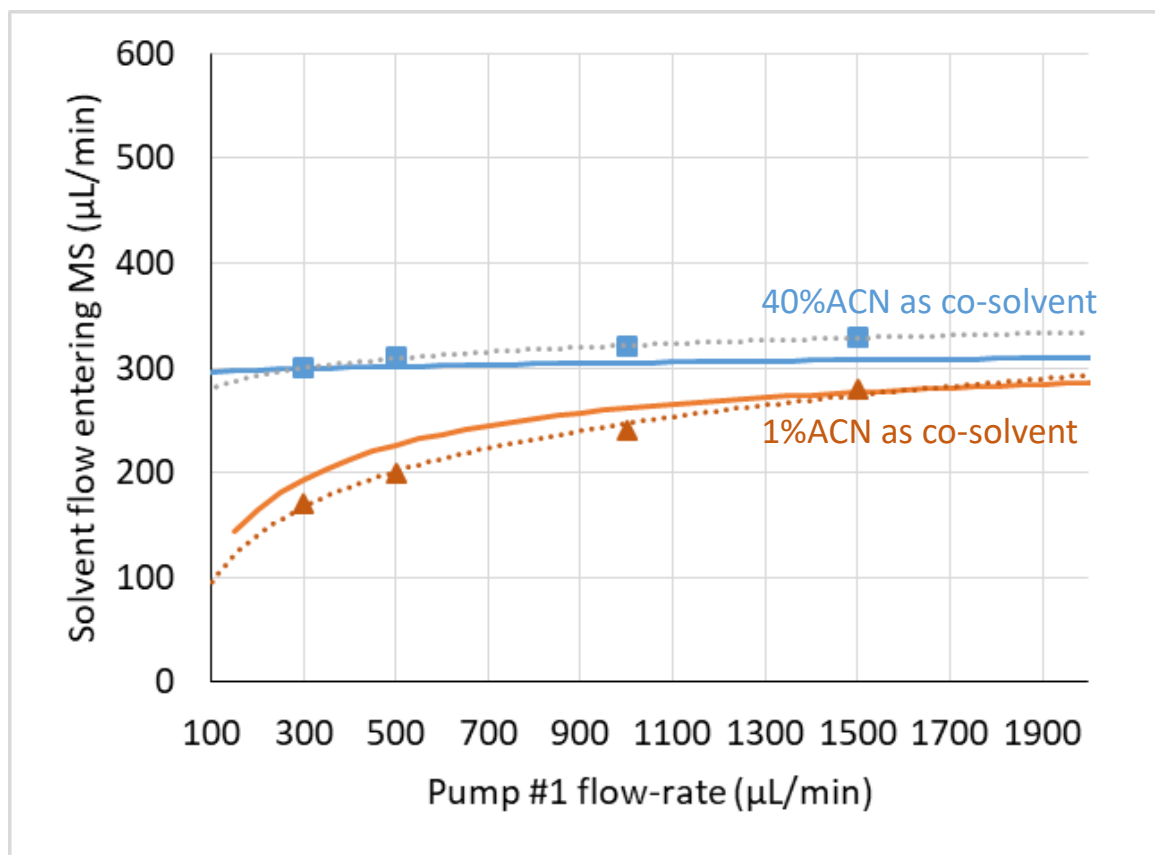


Figure 2

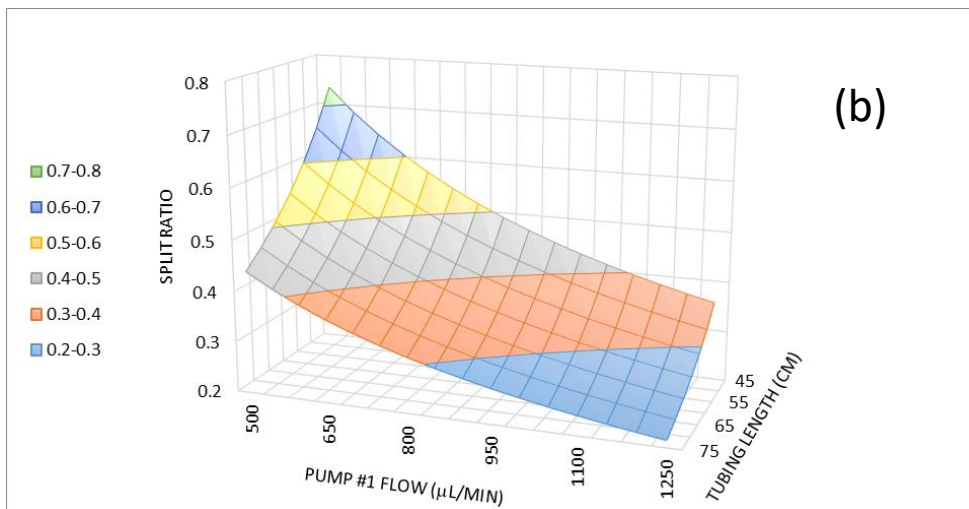
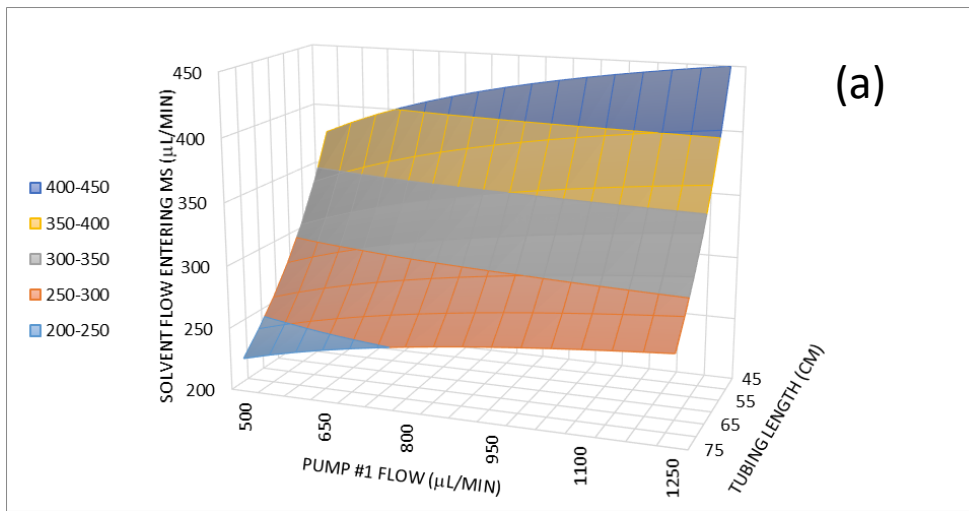


Figure 3

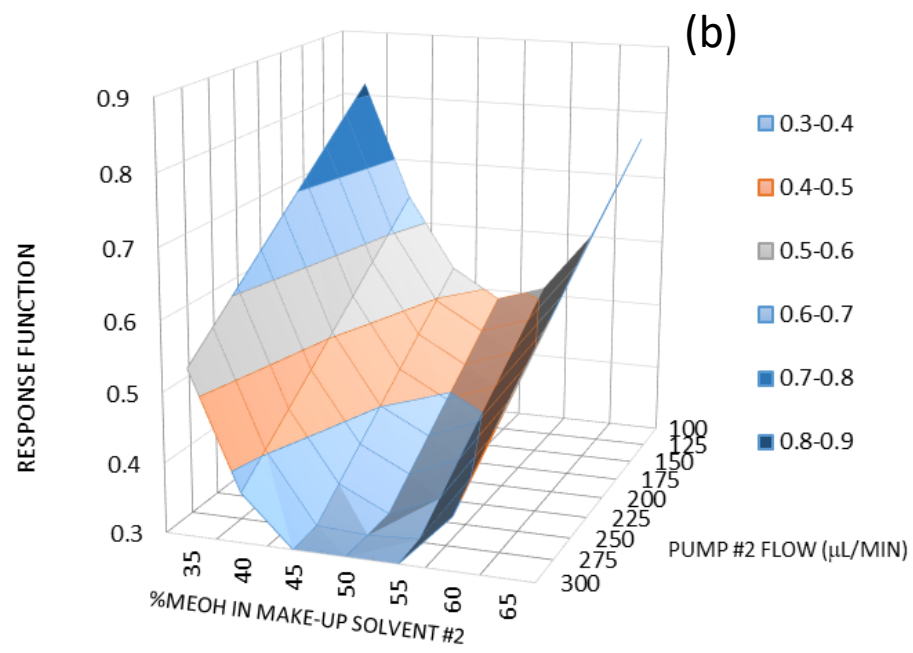
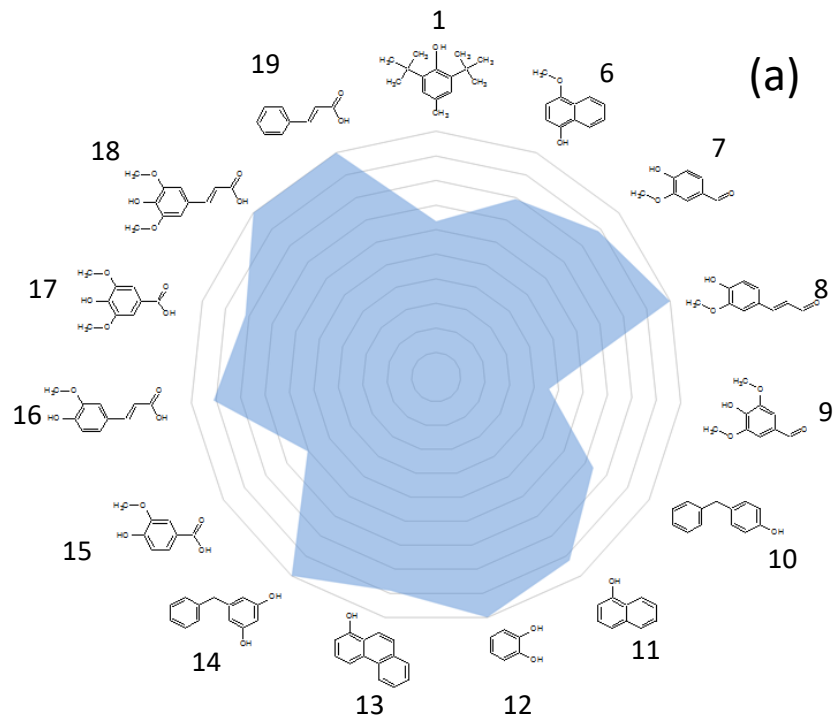


Figure 4

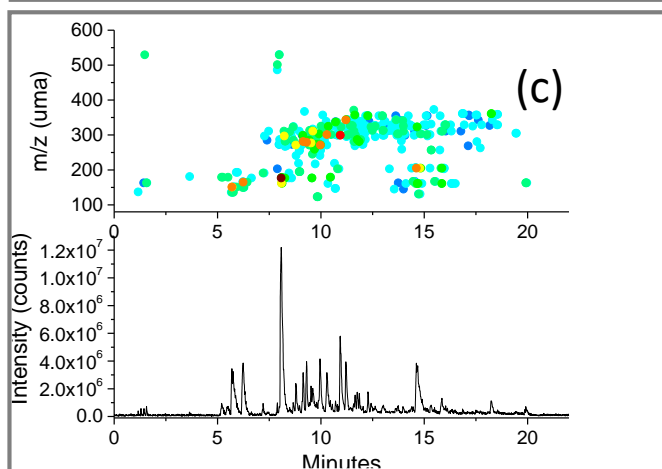
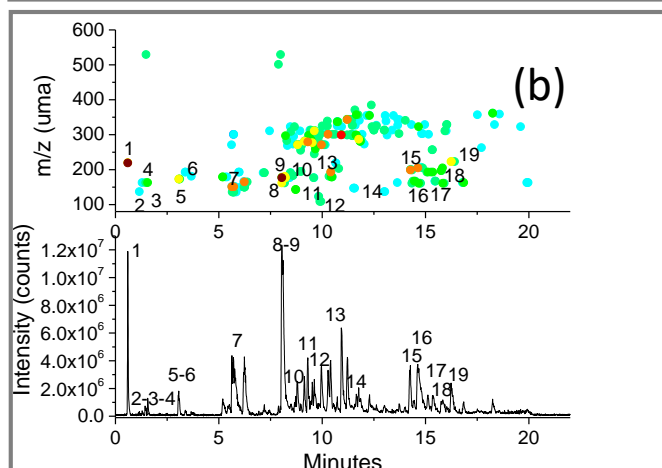
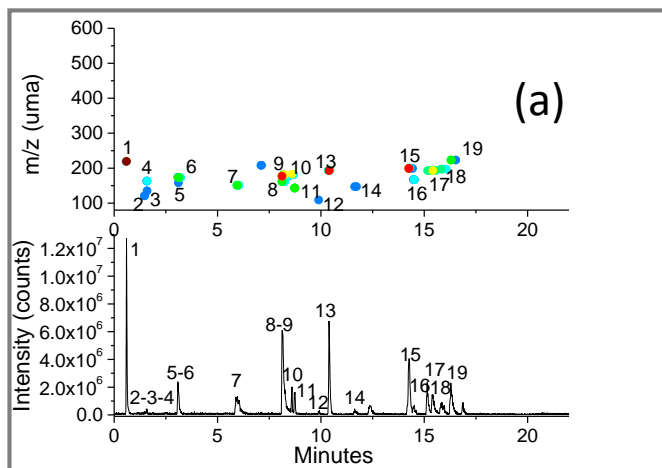


Figure 5

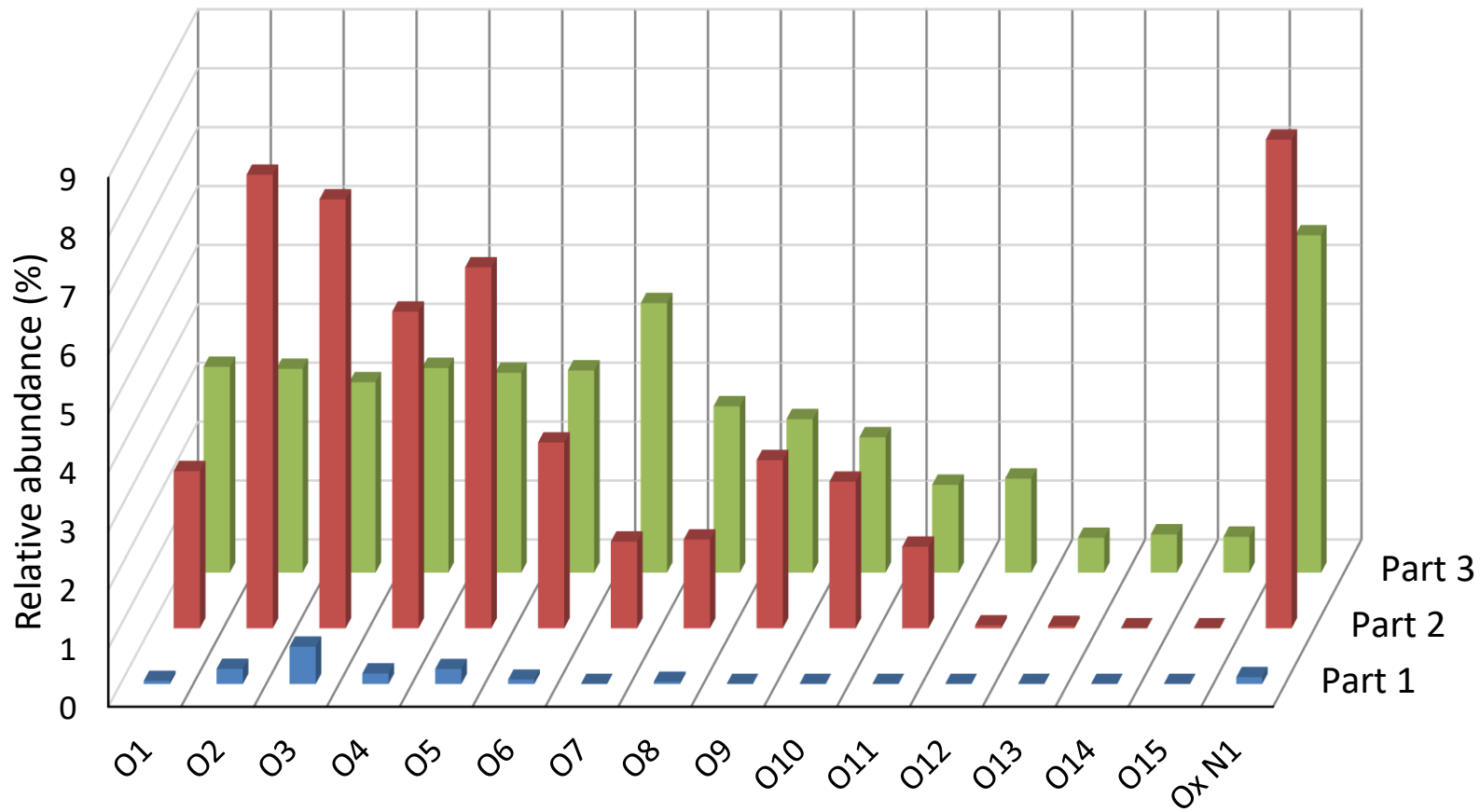


Figure 6

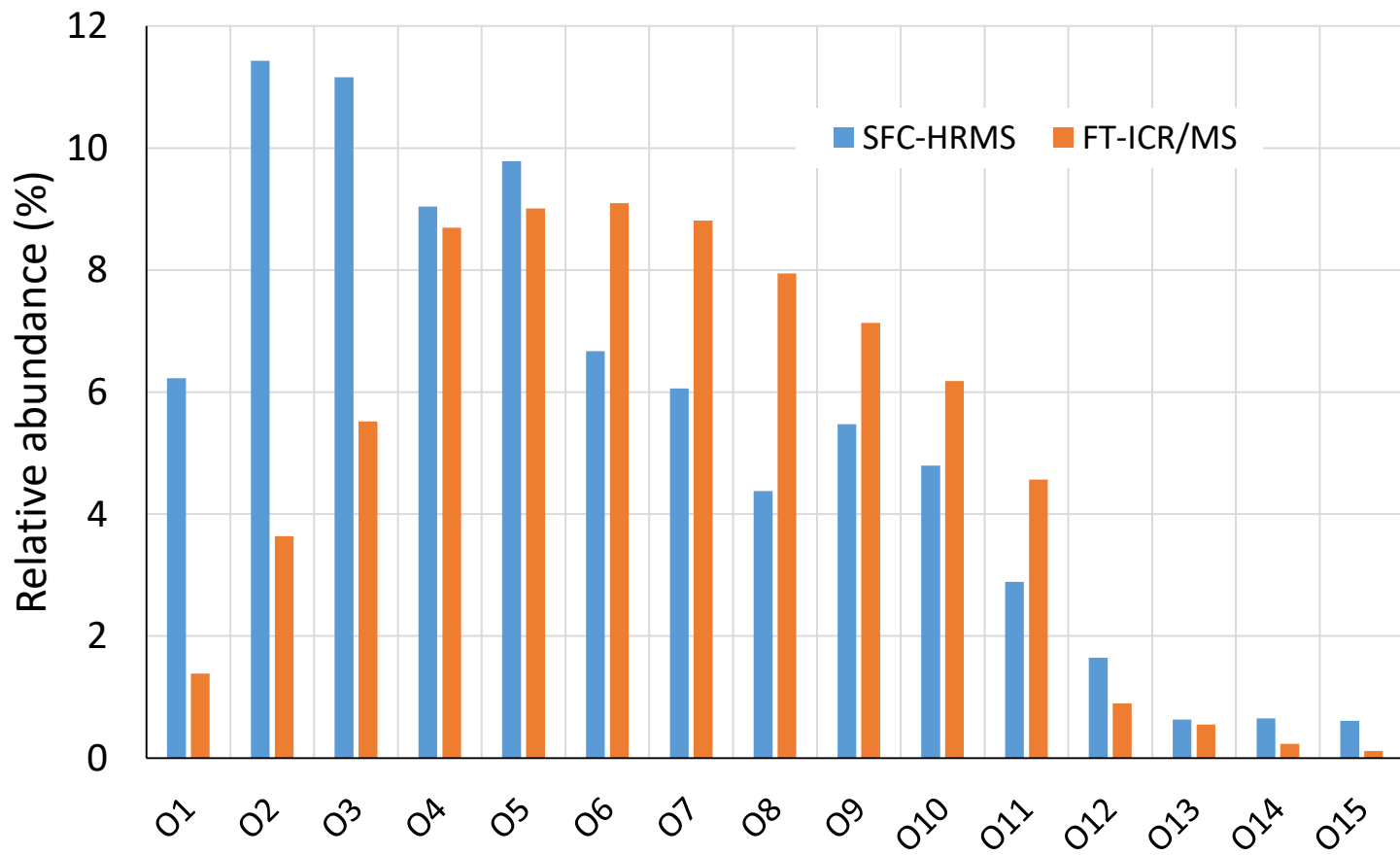


Figure 7

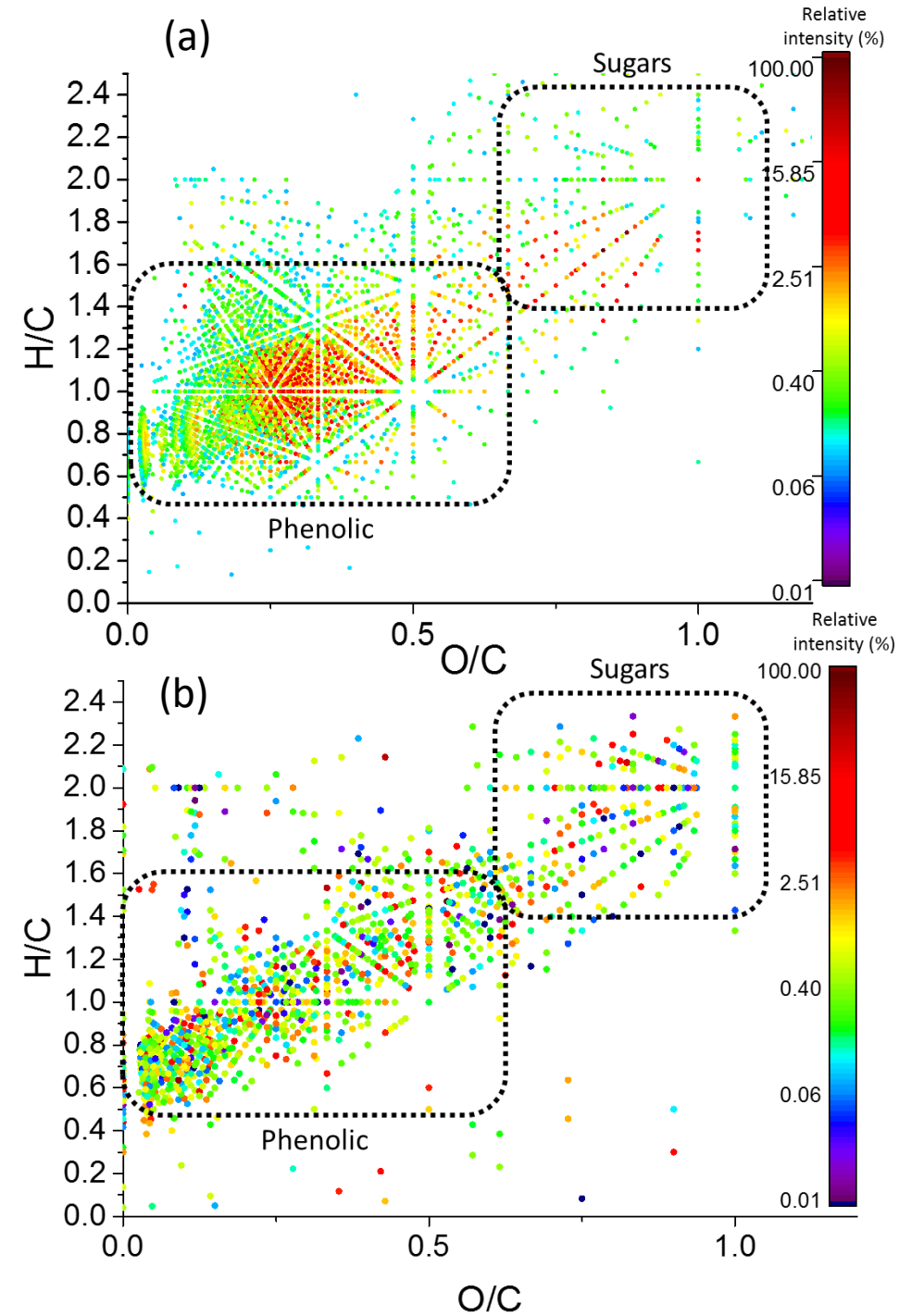


Figure 8

Table 1 : List of 19 (among 36) model compounds detected in SFC(-)APCI-HRMS and their corresponding results obtained from SFC/MS software. See experimental section for SFC and MS conditions.

	IUPAC name	Usual name	Retention time (min)	Accurate weight [M-H]-	Molecular formula	Mass error Δm (ppm)
1	2,6-ditertbutyl-4methylphénol	2,6-ditertbutyl-4methylphénol	0.597	219.1765	C <sub>15</sub> H <sub>24</sub> O <sub>1</sub>	-0.634
2	2,6-Dimethylphenol	Xylenol	1.478	121.0685	C <sub>8</sub> H <sub>10</sub> O <sub>1</sub>	-14.773
3	2,4,6-trimethylphenol	Trimethyl phenol	1.595	135.079	C <sub>9</sub> H <sub>12</sub> O <sub>1</sub>	-19.936
4	2-methoxy-4-[(E)-prop-1-enyl]phenol	Isoeugenol	1.595	163.0792	C <sub>10</sub> H <sub>12</sub> O <sub>2</sub>	-18.015
5	1,3-Dimethoxy-2-hydroxybenzene	Syringol	2.532	153.0582	C <sub>8</sub> H <sub>10</sub> O <sub>3</sub>	8.378
6	2-Methoxy-1-naphthol	Methoxy-naphtol	3.137	173.0628	C <sub>11</sub> H <sub>10</sub> O <sub>2</sub>	19.051
7	4-hydroxy-3-méthoxybenzaldéhyde	Vanillin	6.062	151.0425	C <sub>8</sub> H <sub>8</sub> O <sub>3</sub>	19.414
8	(E)-3-(4-hydroxy-3-methoxyphenyl)prop-2-enal	Coniferaldehyde	8.157	177.0589	C <sub>10</sub> H <sub>10</sub> O <sub>3</sub>	8.937
9	4-hydroxy-3,5-diméthoxybenzaldéhyde	Syringaldehyde	8.217	181.056	C <sub>9</sub> H <sub>10</sub> O <sub>4</sub>	5.345
10	4-Benzylphenol	Hydroxy-diphenylmethane	8.622	183.0841	C <sub>13</sub> H <sub>12</sub> O <sub>1</sub>	13.991
11	Naphtalén-1-ol	Naphtol	8.757	143.0516	C <sub>10</sub> H <sub>8</sub> O <sub>1</sub>	14.412
12	Benzene-1,2-diol	Catechol	9.893	109.03	C <sub>6</sub> H <sub>6</sub> O <sub>2</sub>	-2.779
13	9-Phenanthrenol	Phenantrol	10.438	193.0691	C <sub>14</sub> H <sub>10</sub> O <sub>1</sub>	17.670
14	(2E)-3-Phenylprop-2-enoic acid	Trans-cinnamic acid	11.625	147.0435	C <sub>9</sub> H <sub>8</sub> O <sub>2</sub>	-11.242
15	4-benzylbenzene-1,3-diol	Benzyl-resorcinol	14.3	199.0779	C <sub>13</sub> H <sub>12</sub> O <sub>2</sub>	-9.811
16	4-Hydroxy-3-methoxybenzoic acid	Vanillic acid	14.553	167.038	C <sub>8</sub> H <sub>8</sub> O <sub>4</sub>	-14.861
17	(E)-3-(4-hydroxy-3-methoxyphenyl)prop-2-enoic acid	Ferulic acid	15.418	193.0539	C <sub>10</sub> H <sub>10</sub> O <sub>4</sub>	-8.974
18	4-Hydroxy-3,5-dimethoxybenzoic acid	Syringic acid	15.877	197.0459	C <sub>9</sub> H <sub>10</sub> O <sub>5</sub>	1.792
19	3-(4-hydroxy-3,5-dimethoxyphenyl)prop-2-enoic acid	Sinapic acid	16.3	223.0656	C <sub>11</sub> H <sub>12</sub> O <sub>5</sub>	15.256

Table 2: List of molecular formulae corresponding to model compounds (listed in Table 1) and identified in the bio-oil sample. The difference in retention times allows to assess the degree of fit that a compound found in the bio-oil has relative to a model compound.

<i>Molecular formula (n)<sup>(a)</sup></i>	<i>Accurate mass [M-H]<sup>-</sup></i>	<i>Model compounds</i>		<i>Bio oil sample</i>		$\Delta$ (tr) <sup>(d)</sup> (min)
		<i>tr<sup>(b)</sup></i>	$\Delta m$ <sup>(c)</sup>	<i>tr<sup>(b)</sup></i>	$\Delta m$ <sup>(c)</sup>	
C <sub>10</sub> H <sub>12</sub> O <sub>2</sub> (4)	163.0792	1.59	18.01	1.58	13.16	0.01
C <sub>11</sub> H <sub>10</sub> O <sub>2</sub> (6)	173.0628	3.05	19.05	3.10	17.31	0.05
C <sub>8</sub> H <sub>8</sub> O <sub>3</sub> (7)	151.0425	5.43	19.41	5.49	17.42	0.06
C <sub>10</sub> H <sub>10</sub> O <sub>3</sub> (8)	177.0589	8.11	8.93	8.06	11.76	0.05
C <sub>9</sub> H <sub>10</sub> O <sub>4</sub> (4)	181.0560	8.11	5.34	3.67	15.83	4.44
C <sub>6</sub> H <sub>6</sub> O <sub>2</sub> (12)	109.0300	9.90	2.78	9.90	13.78	0.00
C <sub>14</sub> H <sub>10</sub> O <sub>1</sub> (13)	193.0691	10.44	17.67	19.61	18.07	9.17
C <sub>9</sub> H <sub>8</sub> O <sub>2</sub> (14)	147.0435	11.60	11.24	10.68	11.20	0.92
C <sub>8</sub> H <sub>8</sub> O <sub>4</sub> (16)	167.0380	14.32	14.86	14.39	9.08	0.07
C <sub>10</sub> H <sub>10</sub> O <sub>4</sub> (17)	193.0539	15.42	8.97	5.94	15.89	9.48
C <sub>9</sub> H <sub>10</sub> O <sub>5</sub> (18)	197.0459	15.80	1.79	10.37	11.40	5.43
C <sub>11</sub> H <sub>12</sub> O <sub>5</sub> (19)	223.0656	16.26	15.26	16.31	5.84	0.05

(a) : model compound number (as in Table 1)

(b) : retention times (min)

(c) : mass error (ppm)

(d) : difference in retention times (min) between model compound and similar bio-oil molecular formula

Table 3: List of molecular formulae identified at several different retention times for a fast pyrolysis bio-oil in SFC(-)APCI-HRMS. See experimental section for SFC and MS conditions.

Molecular formula	Retention times (min)				Unitary mass (uma)
C <sub>10</sub> H <sub>10</sub> O <sub>2</sub>	10.34	14.71	16.51		162
C <sub>10</sub> H <sub>12</sub> O <sub>2</sub>	1.56	19.91			164
C <sub>10</sub> H <sub>10</sub> O <sub>3</sub>	8.13	8.46	6.61		178
C <sub>10</sub> H <sub>12</sub> O <sub>3</sub>	5.19	10.47			180
C <sub>11</sub> H <sub>12</sub> O <sub>4</sub>	6.37	14.68			208
C <sub>16</sub> H <sub>16</sub> O <sub>4</sub>	8.78	9.95			272
C <sub>6</sub> H <sub>10</sub> O <sub>5</sub>	14.67	15.84			162
C <sub>20</sub> H <sub>24</sub> O <sub>5</sub>	11.2	13.62	15.33		344
C <sub>8</sub> H <sub>12</sub> O <sub>6</sub>	13.31	15.95			204
C <sub>14</sub> H <sub>18</sub> O <sub>6</sub>	11.62	11.85	17.54		282
C <sub>16</sub> H <sub>16</sub> O <sub>6</sub>	9.9	14.81			304
C <sub>20</sub> H <sub>26</sub> O <sub>6</sub>	16.89	18.24			362
C <sub>7</sub> H <sub>10</sub> O <sub>7</sub>	14.61	14.78	15.8		206
C <sub>12</sub> H <sub>16</sub> O <sub>7</sub>	9.4	16.74			272
C <sub>13</sub> H <sub>20</sub> O <sub>7</sub>	12.15	17.95			288
C <sub>13</sub> H <sub>18</sub> O <sub>8</sub>	12.1	13.19	15.36		302
C <sub>9</sub> H <sub>20</sub> O <sub>9</sub>	8.81	15.01			272
C <sub>12</sub> H <sub>22</sub> O <sub>9</sub>	8.56	10.77			310
C <sub>10</sub> H <sub>20</sub> O <sub>10</sub>	9.12	13.01	14.51	15.7	300
C <sub>10</sub> H <sub>22</sub> O <sub>10</sub>	11.34	13.89	15.19		302
C <sub>11</sub> H <sub>22</sub> O <sub>10</sub>	10.87	12.45	15.58	16.63	314
C <sub>11</sub> H <sub>24</sub> O <sub>10</sub>	11.3	18.24			316
C <sub>12</sub> H <sub>20</sub> O <sub>10</sub>	8.38	10.97	14.65		324
C <sub>12</sub> H <sub>22</sub> O <sub>10</sub>	10.35	12.69	14.34	16.21	326
C <sub>13</sub> H <sub>22</sub> O <sub>10</sub>	10.7	10.77	12.18		338

## **Supplementary information for**

**Ultra-high performance supercritical fluid chromatography hyphenated to atmospheric pressure chemical ionization high resolution mass spectrometry for the characterization of fast pyrolysis bio-oils.**

**AUTHORS :** Julien CREPIER<sup>(a)</sup>, Agnès LE MASLE<sup>(a)</sup>, Nadège CHARON<sup>(a)</sup>, Florian ALBRIEUX<sup>(a)</sup>, Pascal DUCHENE<sup>a</sup>, Sabine HEINISCH<sup>(b)</sup>

*<sup>a</sup>IFP Energies nouvelles, Rond-point de l'échangeur de Solaize, BP 3, 69360 Solaize, France*

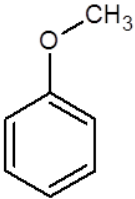
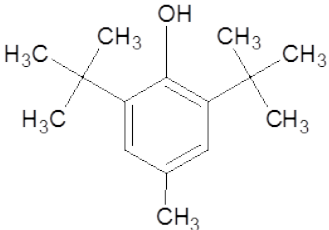
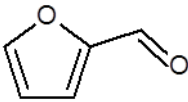
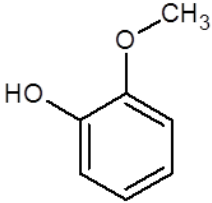
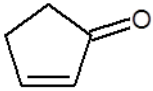
*<sup>b</sup> Université de Lyon, Institut des Sciences Analytiques, UMR 5280, CNRS, ENS Lyon, 5 rue de la Doua, 69100 Villeurbanne, France*

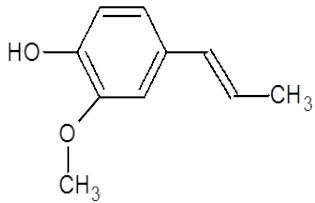
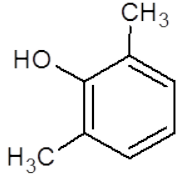
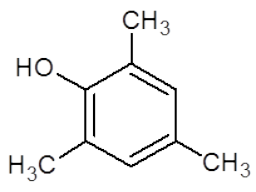
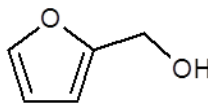
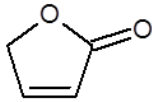
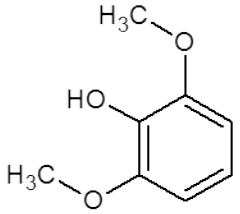
### **CORRESPONDENCE :**

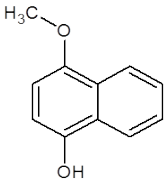
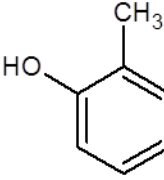
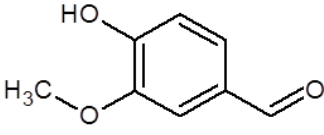
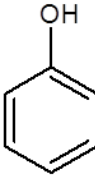
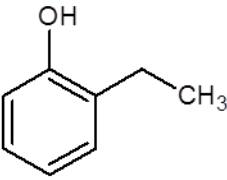
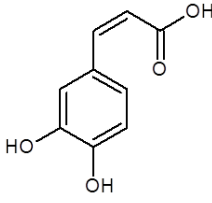
Sabine HEINISCH  
E-mail : [sabine.heinisch@univ-lyon1.fr](mailto:sabine.heinisch@univ-lyon1.fr)  
Phone.: +33 4 37 42 35 51

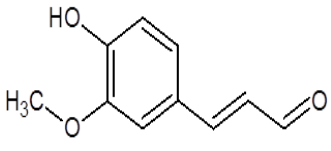
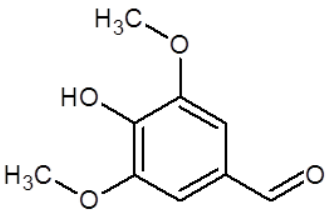
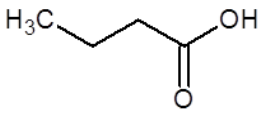
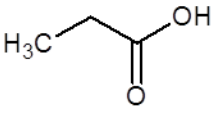
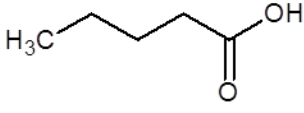
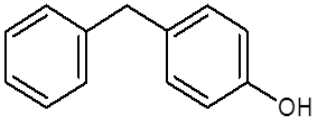
Agnès LE MASLE  
E-mail : [agnes.le-masle@ifpen.fr](mailto:agnes.le-masle@ifpen.fr)  
Phone.: +33 4 37 70 23 91

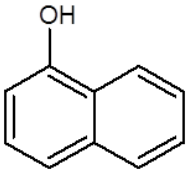
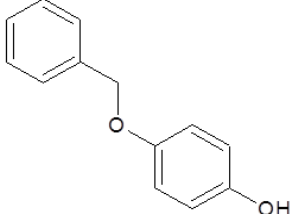
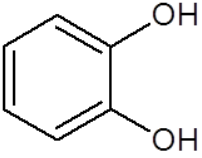
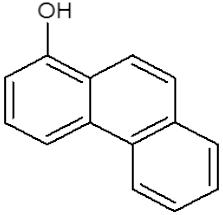
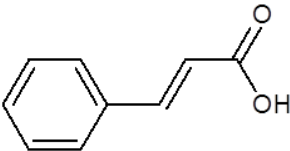
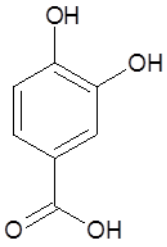
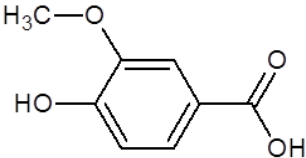
Table S1 : List of the 36 studied model molecules and their characteristics

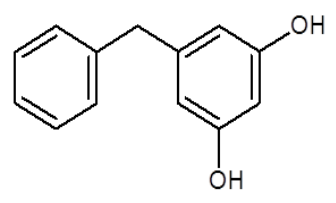
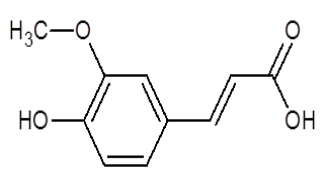
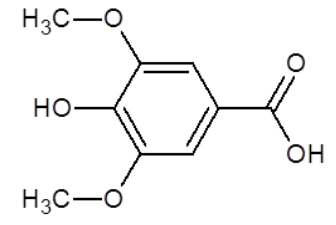
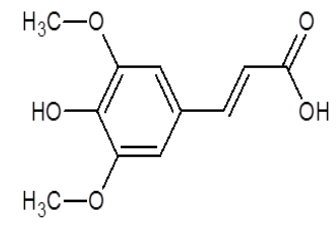
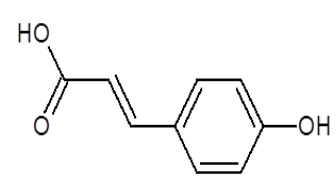
IUPAC name	Structure	C	H	O	Accurate mass (uma)
Furan		4	4	1	68.0262
Anisol		7	8	1	108.0575
2,6-ditertbutyl-4methylphenol		15	24	1	220.1827
2-Furaldehyde		5	4	2	96.0211
2-Methoxyphenol		7	8	2	124.0524
2-Cyclopenten-1-one		5	6	1	82.0419

2-methoxy-4-[(E)-prop-1-enyl] phenol		10	12	2	164.0837
2,6-Dimethylphenol		8	9	1	121.0653
2,4,6-trimethylphenol		9	12	1	136.0888
2-Furylmethanol		5	6	2	98.0368
2(3H)-Furanone		4	4	2	84.0211
1,3-Dimethoxy-2-hydroxybenzene		8	10	3	154.0630

2-Methoxy-1-naphthol		11	10	2	174.0681
(4-Methylphenyl) methanol		7	8	1	108.0575
4-hydroxy-3-methoxy benzaldehyde		8	8	3	152.0473
Phenol		6	6	1	94.0419
2-Ethylphenol		8	10	1	122.0732
acid (E) 3-(3,4-dihydroxyphényl) prop-2-énoïque		9	8	4	180.0423

(E)-3-(4-hydroxy-3-methoxyphenyl) prop-2-enal		10	10	3	178.0630
4-hydroxy-3,5-dimethoxy benzaldehyde		9	10	4	182.0579
Butanoic acid		4	8	2	88.0524
Propanoic acid		3	6	2	74.0368
Pentanoic acid		5	10	2	102.0681
4-Benzylphenol		13	12	1	184.0888

Naphtalen-1-ol		10	8	1	144.0575
4-(benzyloxy) phenol		13	12	2	200.0837
Benzene-1,2-diol		6	6	2	110.0368
9-Phenanthrenol		14	10	1	194.0732
(2E)-3-Phenylprop-2-enoic acid		9	8	2	148.0524
3,4-dihydroxybenzoic acid		7	6	4	154.0266
4-Hydroxy-3-methoxybenzoic acid		8	8	4	168.0423

4-benzylbenzene-1,3-diol		13	12	2	200.0837
(E)-3-(4-hydroxy-3-methoxyphenyl)prop-2-enoic acid		10	10	4	194.0579
4-Hydroxy-3,5-dimethoxybenzoic acid		9	10	5	198.0528
3-(4-hydroxy-3,5-dimethoxyphenyl)prop-2-enoic acid		11	12	5	224.0685
3-(4-hydroxyphenyl)prop-2-enoic acid		9	8	3	164.0473

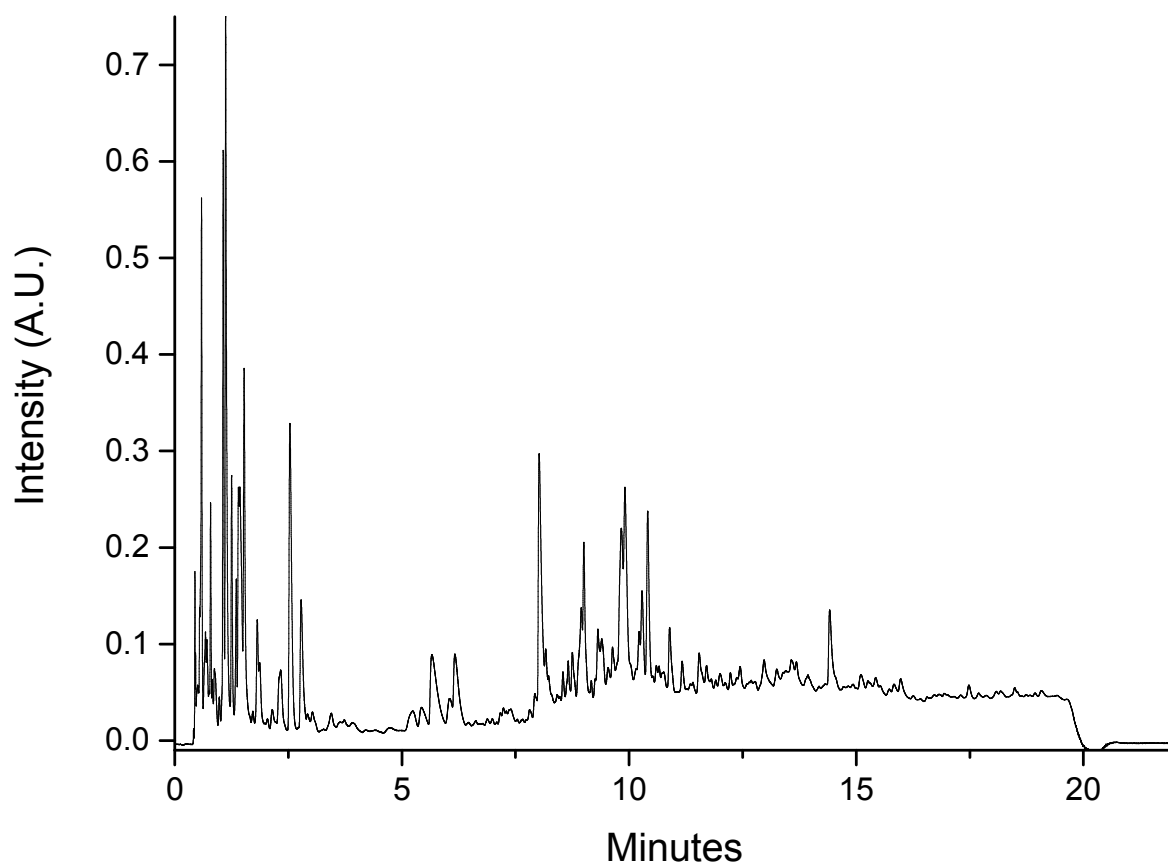


Figure S1 : SFC separation of a fast pyrolysis bio-oil under optimized conditions (stationary phase: Acquity BEH 2-EP, modifier: ACN/H<sub>2</sub>O (98/2), temperature: 30°C, BPR pressure: 150 bar). UV detection (210nm).